A General Pressure Generation Model for Granular Propellant Fires

Dr. Frederick Paquet; General Dynamics – Ordnance and Tactical Systems, Canada, Valleyfield; Valleyfield, Quebec, Canada

Dr. Hoi Dick Ng; Concordia University; Montreal, Quebec, Canada

Mario Paquet; General Dynamics – Ordnance and Tactical Systems, Canada, Valleyfield; Valleyfield, Quebec, Canada

Keywords: fire safety, deflagration, explosion pressure, granular propellants, deflagration venting.

Abstract

Propellants fires can generate pressures that have disastrous consequences for the environment surrounding the event. The main goal of this work is to provide a way to predict the pressure evolution inside a semi-vented enclosure during a propellant fire. A general approach was taken in which the conditions of a semi-confined propellant fire are transcribed into a set of differential equations. In order to verify the validity of the theoretical model and further adjust some of the input parameters, tests were performed in vented enclosures. Several enclosure volumes varying from 60-L to 1800-L were used to check the geometrical scaling effect. Granular propellant of various compositions and geometries were tested. To quantify the unknown variables, an empirical approach was taken where the results of fire tests were analyzed to yield the desired parameters. The general methodology applied involved comparing statistical models derived from the experimental data and fitting the corresponding parameters with the theoretical model. To solve such parameter estimation problems (also known as inverse problems), multivariate regression methods are applied with a proper data regularization scheme. The results are simple model equations with parameters of known values which account for changes in propellant configurations and event scales.

1. Introduction

Propellants are designed to provide mechanical energy through the action of the pressure generated by the transformation of solid grains to a high temperature gas. For that same reason, an unwanted combustion will generate pressures that can have disastrous consequences for the environment surrounding the fire. Propellants at very low densities (small mass in a large volume) can easily generate pressures that far exceed what standard walls can resist. When there is some confinement of the propellant, pressures in excess of 70 kPa can easily be generated at 12 m from the event (Racette, Brousseau and Valliere 2004)

There are very few publications of pressure measurements made with propellant fires in open areas. Test results related to storage areas and naval vessel compartments have been published, but often do not include a theoretical analysis, or cover only certain limited cases (White et al. 2000) (Joachim 1991). A paper by Polcyn and Mullin examined the pressure generation during airbag propellant fires in a 5.3 m^3 vented enclosure (Polcyn and Mullin 1998). An electric detonator located at the bottom of the samples was used to ignite the propellants. Such a configuration can be problematic, as it would generate a large amount of projections and thus yield potentially erratic results. An attempt at modelling explosion pressure venting was made by Graham in cases involving the slow burning of high explosives (such as RDX and Composition B) (Graham 1986). The model involved building a pressure-time derivative equation by taking the difference between a pressure rise and pressure decay term. Each term was determined from basic thermodynamics and gas flow dynamics principles. From the resulting equation, a critical vent area ratio was defined as the solution yielding a pressure-time derivative of zero.

Modelling these types of events was also attempted by Porterie et al. through the use of a fully numerical methodology where the Navier-Stokes equations are solved (Porterie et al. 1996). The model applies thermodynamical and chemical considerations of the combustion to calculate the gas temperature, pressure, velocity and composition in a room. Although it would eventually constitute the most complete approach, it remains complex to use in an industrial setting, given the limited knowledge often available about the propellant combustion characteristics.

Some studies have been made by the industry about the critical height of propellants for detonation in which generated pressures were recorded (Racette, Brousseau and Valliere 2004) (Frauenfelder 1983). These results have not often been published. The pressure data was used to determine if a shock wave was created by the combustion (as a criterion to discern between deflagration and detonation) (Racette, Brousseau and Valliere 2004). A study by Merrifield and Myatt explored the effect of a black powder type propellant fire with quantities and containers comparable to those that could be manipulated by a hunter in his house (Merrifield and Myatt 1998). Although the core of the study focused on the flight of container fragments, the results show various levels of overpressures generated at a given distance from the combustion of a sample (Merrifield and Myatt 1998). In these previous cases, no attempt is made to derive a prediction model for the observed pressures. Many of these studies also focus on cases where the burning sample is initially confined and thus generates pressure waves upon the sudden rupture of the container. The analysis is therefore more akin to that of detonating substances, such as explosives, than it is to that of fire science. A good example is that of the study related to the venting of explosion initiated by fragment impact on cased ammunition (Graham 1986). Comparisons with explosive effects have been made in the measurement methods used and application of the TNT (trinitrotoluene) equivalence concept (Polcyn and Mullin 1998) (Wharton and Formby 2001).

Although propellant fire venting has not been studied rigorously, the explosion venting problem has seen much research performed in the context of various other applications. Combustible gas, vapor and dust mixtures can ignite and generate violent explosions. Oil refineries (Eckhoff 2005) and coal mines (Amyotte 2013) are examples that show that such events can indeed occur in industrial settings and have terrible consequences. As a result of these unfortunate events and through the application of research results, explosion venting guidelines have been published. One of the most known set of guidelines is NFPA 68 by the National Fire Protection Association (NFPA 2010). The NFPA 68 covers various fuels, vent panel masses and building geometries and is applied in many industries.

Even if the mechanisms at play differ in each application, there are some similarities in the mathematical formulation of such problems. Gas and dust explosions both involve a volume filled with a mixture of fuel and oxidant in which a combustion front is travelling. High explosives and confined propellants generate a spatially localized pressure wave which will also travel in the enclosure. Unconfined propellant fires can be compared to having a pressurized tank emptying in the room after opening a valve. In this last analogy, the period between ignition and maximum fire dimension (flame propagation) is equivalent to the valve opening. Albeit their intrinsic differences, all these cases ultimately involve a mixture of pressurized gases flowing through a constriction to an infinite medium at atmospheric pressure. It should thus be expected that the maximum pressure solution follows a similar form.

In the present paper, a general analysis of the propellant deflagration venting problem is attempted. As various gas dynamic modelling schemes are possible, the thermodynamic aspect of the problem is initially treated. From these basic considerations, a theoretical model is derived. The model is based on a fundamental differential equation and specific solutions applicable to the problem. A numerical solution scheme is also presented, as the methodology is useful in inferring some of the thermodynamic properties of the combustion gases. The results of small and medium scale experimental tests are then presented. Statistical methods are used to analyze the results and link them to the theoretical model. Comparisons are also performed between the theoretical, numerical and empirical methods in order to validate the results. It must be noted that a more detailed account of this work was published in the form of a doctoral dissertation by the main author (Paquet, 2017).

2. Theoretical model

2.1 General considerations

By design, propellant is manufactured to eventually be used by applications requiring large impulses. The mechanical energy required for these impulses comes from the rapid transformation of solid propellant to gaseous products during combustion. For example, it is known that an ideal gas will be at standard temperature and pressure (STP, or ambient conditions) when each mole of gas occupies 22.4 L. The average molecular weight of propellant combustion gases is in the 20 to 30 g/mol range and quantities in the kilogram range are most often handled. It is thus observed that small amounts of propellants can generate important pressures in a closed space.

An important concept used in determining the thermodynamic behaviour of the propellant gases is that of the equation of state. Such an equation is used to relate the thermodynamic variables such as pressure, P, volume, V, and temperature, T, for a given substance. The ideal gas law is an example and perhaps the simplest equation of state. In the ideal gas law, the three thermodynamic variables are related through the gas quantity, N, and the ideal gas constant, R = 8.314 kJ/kg K (Cengel and Boles 2014). In the case of propellant combustion, the Nobel-Abel equation is usually applied in calculations. This last relationship is expressed as:

$$P\,(V - b) = NRT \qquad \textit{Eq. 1}$$

where b is known as the covolume of the combustion gases. The covolume accounts for the departure from an ideal gas behaviour due to the non-negligible interaction between molecules, an effect here modelled as a loss in volume. Typical propellants have covolume values around 1 mL/g. For a 200 ml closed vessel containing 10 g of propellant, this represents a volume loss of 10 mL, or 5% of the total available volume. In the case of a 1000 kg sample in a 1000 m^3 room, the volume loss is 1000 L, or 0.001% of the total volume. It can thus be observed that the effect of the covolume is negligible for cases involving small mass to volume ratios (denoted as the charge density, c). With a covolume of 1 cc/g, the volume loss over total volume ratio is indeed equal to the charge density. Assuming that a volume loss of less than 1% is negligible implies that cases where the charge density is less than 0.01 g/mL can be treated using the ideal gas law. Alternatively, for propellants with a covolume differing from 1 mL/g, a dimensionless quantity defined as the ratio of the charge density over the covolume can be computed:

$$X = c\,b \qquad \textit{Eq. 2}$$

The use of the Nobel-Abel equation of state is thus warranted when $X >> 0.01$. The ideal gas law can be used for all other cases.

To correctly model the dynamic pressure behaviour in a given situation, it is necessary to determine if spatial variations are expected within a domain. In most cases, a domain shall be defined as the volume of an enclosure. As gases are generated at the location of the fire, the surrounding air shall be compressed and subsequently mixed with the combustion products. The compression wave will travel through the enclosure volume at the sound velocity corresponding to the air conditions. Depending on the gas generation rate, the magnitude of the compression wave will vary. In addition, a higher magnitude wave will reflect on the enclosure boundaries and generate dynamic effects. At the limit, for a slow enough event and large enough enclosure, the time required for the small compression wave to travel through the enclosure shall be negligible compared to the event time scale. In such a case, it will be advantageous to consider the entire enclosure volume as a lump with conditions that do not depend on spatial dimensions. This last situation is known as a lumped parameter problem and mathematical conditions must be determined to define the applicability of this case.

Considering a symmetrical enclosure with characteristic distance d (for example, in a cubical enclosure, d would be equal to half the size of any side) filled with mass m_a of air at STP conditions. A gas source located at the base center of the enclosure generates combustion products at a rate $\dot{m}_{gen}$ in kg/s. The goal is to compare both the compression wave travel time to the enclosure dimension, and the generated gas quantity to the “potential” of the enclosure. By arranging the relevant variables together, a dimensionless expression containing ratios describing the previously discussed relationships can be formed. The following dimensionless quantity is thus defined as follows:

$$\chi = \frac{m_{air} c_{air}}{\dot{m}_{gen} d} \quad \text{Eq. 3}$$

Computation of χ with several typical cases is shown on Table 1. It can be concluded that the lumped parameter methodology can be safely used when $\chi >> 1$ as closed vessel modelling has been shown to be fairly precise (Carlucci and Jacobson 2013). This represents most of the cases covered in the present work. The present dimensionless quantity is similar to the often used Biot Number in heat and mass transfer problems (the Biot number gives a measure of the capacity of a body conduct heat / mass within itself when heat / mass is being convected at its surface).

Table 1: Estimated χ values for a variety of cases.

Case	χ (dimensionless)
0.7 L closed vessel with a fast burning propellant	0.9
0.7 L closed vessel with a slow burning propellant	5.6
60 L tank with a fast burning propellant	420
1800 L enclosure with a fast burning propellant	561
10^6 L enclosure with a fast burning propellant	675

The evolution of pressure inside an unvented enclosure due to a propellant fire can thus be computed using the ideal gas law in a lumped parameter setting with a gas generation model which fits the event in question. If venting is added into the picture, a mass loss term must be added into the equations to account for the vented gas. The determination of the mass loss can be performed either with or without the assumption of incompressible flow. The choice of assuming compressibility is made using the known criterion for these cases. The criterion is based on knowledge of the Mach number (ratio of the gas velocity over the sound velocity in the medium) for the flow in question. The Mach number can be calculated using the known pressure ratio between the interior and exterior of the enclosure (John and Keith 2006). In the presently discussed isochoric conditions, flows with a velocity below Mach 0.30 can be simplified as incompressible and the Bernoulli equation applied:

$$v = \left(\frac{2P}{\rho_{gas}}\right)^{1/2} \quad \text{Eq. 4}$$

For Mach numbers above 0.30, compressibility must be taken into account through the use of isentropic relationships (John and Keith 2006).

2.2 Pressure evolution model

In order to devise a pressure evolution model, mass conservation is used. Performing a mass balance on the enclosure volume yields:

$$\dot{m}_e = \dot{m}_{gen} - \dot{m}_{vent} \quad \text{Eq. 5}$$

As discussed previously, the vented mass flow rate can be obtained by applying the Bernoulli equation to compute the gas flow velocity. The vented mass flow rate is thus:

$$\dot{m}_{vent} = C_D \rho_{gas} v A = C_D A \left(2 \rho_{gas} P\right)^{1/2} \quad \text{Eq. 6}$$

where C_D is the discharge coefficient. Using the ideal gas law, the pressure factor can be replaced by a mass dependent factor:

$$\dot{m}_{vent} = C_D A \left(\frac{2 \rho_{gas} m_e R T}{M_w V}\right)^{1/2} \quad \text{Eq. 7}$$

Substituting in the mass balance relation and rearranging the equation yields the following result:

$$\dot{m}_e + C_D A \left(\frac{2\rho_{gas} RT}{M_w V}\right)^{1/2} m_e^{1/2} - \dot{m}_{gen} = 0 \qquad \text{Eq. 8}$$

Assuming that the combustion rate, temperature and density are constant, this is a nonlinear first order ordinary differential equation. This assumption is only necessary in finding analytical solutions to the problem. In the case of numerical solutions, these parameters can be updated as the calculation evolves. Given the finite amount of propellant burning, the $\dot{m}_{gen}$ term will be nonzero when $0 \leq t \leq t_{burn}$. Two cases are thus possible:

$$\dot{m}_e + C_D A \left(\frac{2\rho_{gas} RT}{M_w V}\right)^{1/2} m_e^{1/2} - \dot{m}_{gen} = 0 \qquad \text{when } 0 \leq t \leq t_{burn} \qquad \text{Eq. 9a}$$

$$\dot{m}_e + C_D A \left(\frac{2\rho_{gas} RT}{M_w V}\right)^{1/2} m_e^{1/2} = 0 \qquad \text{when } t > t_{burn} \qquad \text{Eq. 9b}$$

The solution for the first case is difficult, as it requires using the Lambert special function. It is, however, possible to use the differential equation to determine the maximum pressure and the largest rate of pressure change. This analysis will be performed in the next sections. For the second case, the problem reduces to solving a separable first order differential equation.

2.3 Maximum pressure

From the previous differential equation, the maximum pressure can be determined by setting $\dot{m}_e = 0$ and solving for m_e. After some algebra, this yields the following:

$$m_e = \frac{\dot{m}_{gen}^2 M_w V}{2C_D^2 \rho_{gas} RT A^2} \qquad \text{Eq. 10}$$

Using the ideal gas law, the maximum pressure is calculated as:

$$P_{max} = \frac{\dot{m}_{gen}^2}{2C_D^2 \rho_{gas} A^2} \qquad \text{Eq. 11}$$

This constitutes the most general form of the solution for the maximum pressure inside a vented enclosure with the assumptions made. Any further simplification would involve finding an appropriate model for the factor $\dot{m}_{gen}$. One must, however, be careful in choosing an approximation for $\dot{m}_{gen}$, as the model choice will be highly dependent on the case configuration. The following general result is thus obtained:

$$P_{max} = f\left(\frac{\dot{m}_{gen}^2}{A^2}\right) \qquad \text{Eq. 12}$$

A result that is similar to the general form of models found in the literature and discussed previously:

$$P_{max} = f\left(\frac{r^2 S^2}{A^2}\right) \qquad \text{Eq. 13}$$

Here, the difference is seen to be strictly in the numerator of the two expressions. These expressions become nearly identical if, for example, it is assumed that the gas generation rate is simplified as $\dot{m}_{gen} \approx Sr\rho_{bulk}$ where ρ_{bulk} is the bulk density of the propellant. Such a mass combustion model would be akin to the case of a propellant in a container with surface area *S*, burning from the top down. One can observe here that this last statement contains several assumptions: top ignition, constant surface area, laminar vertical propagation through the propellant bed. The problem is that propellant combustion is seldom that ideal. The most general solution therefore remains the best start point for further analysis.

2.4 Maximum rate of pressure rise

Starting with Eq. 9, the maximum value of the mass rate of change derivative can be obtained by differentiating the equation and setting the second mass derivative equal to zero as follows:

$$\ddot{m}_e = \frac{1}{2} A_D \left(\frac{2\rho_{gas} RT}{M_w V}\right)^{1/2} m_e^{-1/2} \dot{m}_e = 0 \qquad \text{Eq. 14}$$

It can be seen that the maximum occurs when *m(t)=0,* which is at *t=0* in this case. The maximum rate of change of the mass is thus:

$$\dot{m}_{max} = \dot{m}_{gen} \qquad \text{Eq. 15}$$

Transforming the last result to the pressure equivalent yields:

$$\dot{P}_{max} = \frac{\dot{m}_{gen} R \Delta T}{M_w V} \qquad \text{Eq. 16}$$

Here again, a proper flame propagation model is important in obtaining a precise value for $\dot{P}_{max}$. The other variables can be calculated using standard thermodynamic methods.

3. Experimental work

3.1 Test setup

In order to study the effect that varying the propellant configuration has on the pressure during a fire, tests were performed in vented enclosures. Enclosure volumes varying from 60 L to 1800 L were used in this study to check the geometrical scale effect. Two sizes of combustion chambers were used:

- Cylindrical 60-L steel reservoir previously used for airbag deployment simulations (cylinder with a radius of 40 cm and a length of 50 cm). A fixed circular opening with a diameter of 1.1 cm (thus an area of 0.0001 m^2) was part of this setup.

- Cubical 1800-L steel plated wooden box (cube with a side length of 122 cm). Openings of various sizes up to 0.40 m^2 could be used on one face of the enclosure.

All pressure measurements were made using Omega pressure transducers (PX309 series). These transducers were located at the centre of every lateral face of the rectangular chambers and on top of the cylindrical enclosure. Measured maximum pressures varying between 15 and 200 kPa, depending on the specific model, could be obtained with these sensors. The measurement range was selected based on the results of preliminary tests in a closed vessel in order to maximize the precision. A 12V DC source was used to power the transducer and the output signals were recorded on a Measurement Computing PMD-1608F data acquisition card, at a rate of 1 kHz. The acquisition was controlled by a laptop through the MCCDAQ software which generated ASCII files containing the pressure measurements.

Table 2: Description of the propellants used in the 60-L and 1800-L tests.

Propellant	Heat of explosion (J/kg)	Composition
SB1	3871	NC: 98% / Inert: 2%
SB2	3135	NC: 90% / Inert: 10%
DB1	5392	NC: 60% / NG: 39% / Inert: 1%
DB2	4490	NC: 73% / NG: 25% / Inert: 2%

Table 3: Tested propellants physical description.

Propellant	Geometry	Grain diameter (mm)	Abs. density (kg/m^3)	Bulk density (kg/m^3)
SB1	Unitubular	0.89	1550	950
SB2	Unitubular	1.17	1590	810
DB1	Disc	0.12 (thickness)	1600	550
DB2	Unitubular	1.16	1590	970

Various propellant types were used and their summary description can be found in Tables 2 and 3. It must be noted that single base propellants use nitrocellulose (NC) as the only energetic component while double bases use a combination of nitrocellulose and nitroglycerin (NG). The heats of explosion shown in Table 2 were measured with a bomb calorimeter in an inert atmosphere.

For all cases, the granular propellant sample was placed in a small container at the centre of the enclosure base. Ignition of the propellant was done using a nichrome hot wire connected to a 25V DC battery. Since contact with the hot wire was enough to ignite the tested propellants, the wire was always laid on the top centre of the sample. For safety reasons, the ignition circuit contained an interlocking mechanism enabling the person in charge to disable its operation during manipulations. The general procedure used during all tests was as follows:

1. Installation of the setup.
2. Closing all necessary roads and sending a radio announcement about the testing.
3. Disabling the ignition circuit.
4. Installing the propellant sample.
5. Closing the enclosure with the proper vent opening.
6. Starting the data acquisition.
7. Moving to a safe distance.
8. Enabling the ignition circuit.
9. Igniting the material and waiting for the end of the event (typically 20-30 s).
10. Stopping the data acquisition and saving the created datafile.
11. Opening the enclosure (in the case of a mis-fire, a waiting time of 5 min was observed prior investigating the source of the problem).
12. Extinguishing any remaining cinders in the setup using a small amount of water.
13. Repeating steps 3 - 12 for the number of tests required.
14. Reopening the roads and sending a radio announcement about the end of testing.
15. Cleaning and storing all equipments.

For any experimental measurement, it is important to have an idea of the uncertainty of the readings. This can be done by performing repetitive trials and looking at the standard deviation of the results (Taylor 1997). For the types of tests involved in the present work, it would have been difficult to perform repetitive trials on every configuration tested due to economical and time constraints. Repetitions were, however, performed on a single typical case to get an estimate of this uncertainty. The test case was a configuration using 1000 g of small web double base (DB1) in the 1800-L enclosure with an opening of 0.093 m^2. Table 4 contains a summary of the results for the six repetitions performed. The data shows that a fairly important variation is obtained between seemingly identical tests. For example, the maximum pressure varies from 2.16 to 4.66 kPa, yielding a 33% relative standard deviation. One must thus expect a certain amount of variation in the data when looking for trends.

Table 4: Results of six repetitions involving 1000 g of small web double base in the 1800-L enclosure with a venting area of 0.093 m^2.

Repetition	Max. pressure (kPa)	Ind. time (s)	Max. time (s)
1	4.66	0.15	0.37
2	3.74	0.29	0.48
3	5.65	0.35	0.50
4	2.81	0.32	0.57
5	2.91	0.14	0.52
6	2.16	0.26	0.57
Average	3.77	0.25	0.52
Abs. standard deviation	1.23	0.09	0.09
Rel. standard deviation	33%	35%	17%

3.2 Flame propagation in enclosure tests

Using the pressure data obtained in vented enclosure tests, it is possible to extract the type of flame propagation behaviour that occurs during the fires. There are two main possibilities:

- Laminar burning of the propellant bed in the horizontal and vertical direction.
- Simultaneous combustion of all the propellant grains.

The first case was well documented in a previous section and requires using orthogonal flame propagation rate components (horizontal and vertical). For example, cylindrical containers of equal diameters and height h_1 and $h_2 = 2h_1$ would contain masses of m_1 and $2m_1$, respectively, but yield the same mass generation rate as that rate would only depend on the surface area. In this instance, a top ignition is required. As discussed previously, the steady state portion of the combustion will either be in the horizontal or vertical direction. The time required to reach steady state is defined as the induction time.

There are a few configurations available within the dataset which behave in a manner similar to the previous example. Configurations A2, A4 and C4 (in the 1800-L enclosure) were tests done in a smaller diameter container. It is observed that the maximum pressures obtained in these instances were all lower than those obtained with the same configuration in the larger container. For these three occurrences, the mass generation rate and induction time would differ. Given the larger height of the samples compared to their width, the main propagation mode is the vertical velocity, r_y.

The second case is more complex as there will still be a non-negligible time required for the flame to propagate in the entire charge. Again, this initial time will be defined as the induction time. Following the induction time, the combustion will be driven by the propellant linear burning rate and the grain geometry. In this eventuality, a larger sample mass will imply a larger gaseous mass generation rate and the sample diameter will not be an important factor. This case could be observed with top, bottom or internal ignition. It must be noted that since the entire charge will be burning, it is quite likely that propellant grains shall be projected due to their presence in the convective flow.

A set of common pressure - time traces are shown in Figure 1 for fires involving two masses of double base propellant (DB1) in the 1800-L enclosure. From these pressure curves, the events can be decomposed into the following stages:

1. Flames spread until a steady state is reached. This is defined here as an induction time and is apparent by the non-linear section found between 0.0 and 0.3 seconds in Figure 1.

2. Steady state gas generation and venting (gas generation more important). Once either the edge or bottom center of the stack has been reached by the flames (depending on the stack dimensions), the gas generation

rate stays constant. This is thus equivalent to the linear section comprised between 0.3 and 0.5 seconds in Figure 1.

3. Steady state gas generation and venting (gas generation and venting in the same order). In that region the pressure is such that the vented gases rate becomes similar to the generated gases rate. It is not a true steady state since the combined effect of the source and vent yields an oscillatory behavior. In Figure 1, this section occurs between times of 0.5 and 0.8 seconds.

4. At the end of the combustion, the gases vent outside, returning the pressure to the atmospheric value. When all the propellant has been consumed, the gas generation rate decreases to zero and enables the venting to reduce the pressure. This pressure drop can be found after 0.8 seconds in Figure 1.

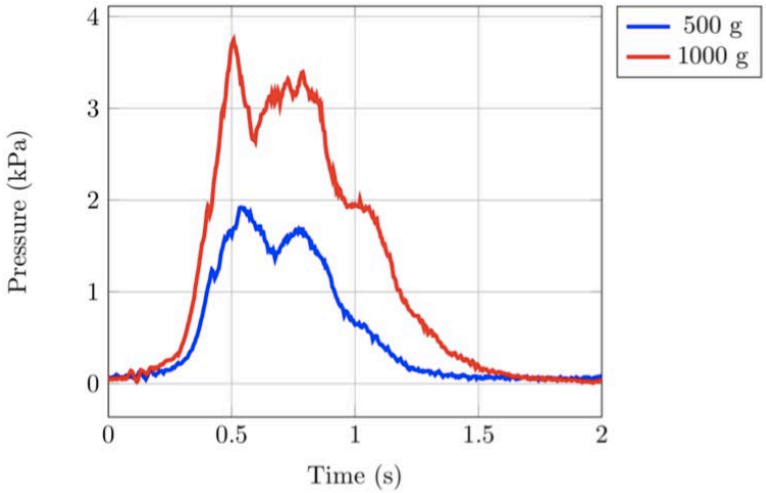

Figure 1: Pressure rise in a vented 1800-L enclosure.

Although the aforementioned sequence applies to all cases, it is important to note that depending on the configuration, some stages might not apply. For example, a stack with dimensions and flame propagation velocities such that the edges and bottom are reached by the flames simultaneously would not exhibit as much of a steady state period (stages 2 and 3). Another example is that of a sample arranged such that the steady state gas generation is large enough to overcome the venting effect. This last case would not exhibit stage 3 and an example is shown in Figure 2. The abrupt pressure drop exhibited in Figure 2 can also occur when a vent panel is used, or if the enclosure suffers any kind of mechanical failure.

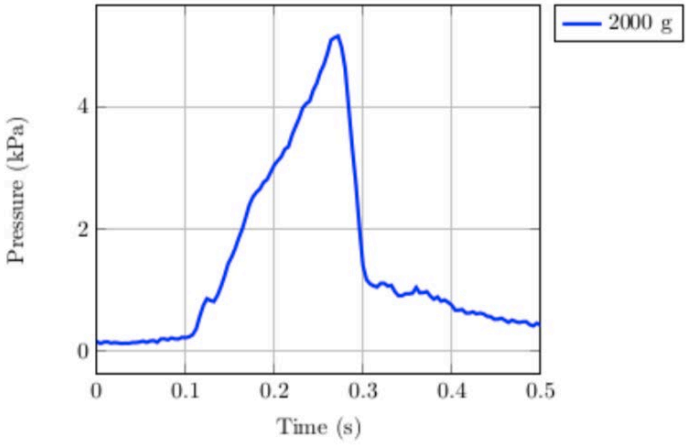

Figure 2: Pressure rise in a vented 1800-L enclosure without the “stage 3” steady state.

An interesting part of the interpretation given above is that one can define a quantity equal to the time required to complete stage 1. This quantity was previously called the induction time and informs about the time required for the flames to propagate such that a steady state is reached. For example, propellant kept in an open container would ignite and the flames would quickly spread on the surface. Once the entire surface is burning, the gas generation is governed by the vertical propagation rate and a linear behavior is observed. Propellants with similar horizontal and vertical propagation rates or stacks of negligible height would not feature an important linear pressure rise section.

In the current case, the measured induction times are nevertheless shown in Tables 5 and 7 for the 60-L and 1800-L configurations. From Table 7, one can observe that configurations A2 and A4 have a noticeably smaller and similar induction time. This is expected as these two configurations have a smaller diameter (smaller container). The following general conclusions can thus be drawn from the available data:

- The induction time depends on the propellant bed diameter.
- The induction time depends on the propellant type (or burning rate).
- If the previous two properties are held constant, the induction time remains constant.

The previous conclusions can be observed graphically by plotting the induction time measured for each test, as shown in Figure 3. The tests performed in the 60-L tank show an evolution of the induction time with each type of propellant tested. The 1800-L induction times are all fairly similar (with the exception of the two smaller diameter cases discussed previously).

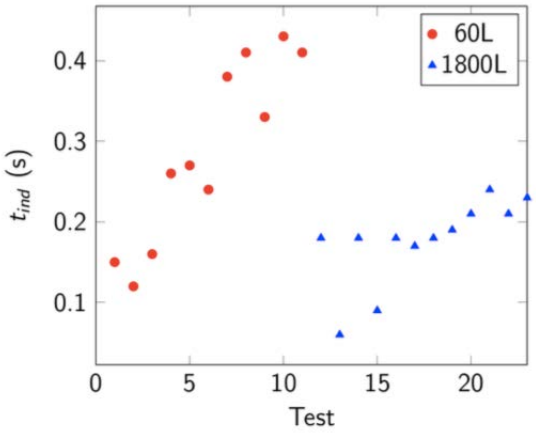

Figure 3: Distribution of measures t_{ind} for all tests.

3.3 Maximum pressures

The 60-L configurations and maximum pressures obtained are given in Table 5. A description of all tested 1800-L configurations along with the maximum pressures obtained are shown in Tables 6 and 7 respectively. The next step is to fit the data with a proper model.

Table 5: Configurations and results summary of the 60-L enclosure tested configurations. This enclosure has a single venting opening area of 0.0007 m^2.

Config.	Propellant	Mass (g)	Max. pressure (kPa)	Ind. time (s)	Max. time (s)
A1	DB1	2.5	9.6	0.15	0.39
A2	DB1	5.0	17.1	0.12	0.41
A3	DB1	10.0	58.7	0.16	0.35
B1	DB2	2.5	8.2	0.26	0.58
B2	DB2	5.0	21.9	0.27	0.59
B3	DB2	10.0	66.7	0.24	0.55
C1	SB1	10.0	9.6	0.38	0.64
C2	SB1	20.0	27.1	0.41	0.77
C3	SB1	30.0	47.0	0.33	0.99
D1	SB2	10.0	2.7	NA	NA
D2	SB2	20.0	23.8	0.43	0.85
D3	SB2	30.0	46.6	0.41	0.85

Table 6: Description of the 1800-L enclosure tested configurations. Note that the stack heights are estimated values from measured diameters and bulk densities.

Config.	Mass (g)	Opening area (m^2)	Stack diameter (m)	Stack height (mm)
A1	50	0.016	0.30	2
A2	50	0.016	0.15	4
A3	100	0.016	0.30	4
A4	100	0.016	0.15	8
A5	150	0.016	0.30	6
B1	150	0.041	0.30	6
B2	177	0.041	0.30	7
B3	250	0.041	0.30	10
C1	250	0.093	0.30	10
C2	500	0.093	0.30	20
C3	1000	0.093	0.30	40
C4	1000	0.093	0.15	80

Table 7: Results summary of the tested 1800-L enclosure configurations.

Config.	Max. pressure (kPa)	Ind. time (s)	Max. time (s)
A1	3.34	0.18	0.54
A2	2.78	0.06	0.40
A3	7.03	0.18	0.48
A4	3.07	0.09	0.40
A5	6.28	0.18	0.42
B1	2.34	0.17	0.53
B2	2.66	0.18	0.42
B3	4.13	0.19	0.43
C1	1.13	0.21	0.31
C2	3.14	0.24	0.50
C3	4.47	0.21	0.65
C4	3.38	0.23	0.49

It is instructive to notice that there is a relationship between the propellant masses and maximum pressures obtained. This relationship is shown in Figures 4 and 5 for the 60-L and 1800-L cases, respectively. In the 1800-L case, the plot shows several opening areas while the 60-L plot shows four propellant types (since the 60-L vent opening size could not be modified). In both cases, a linear trend can be observed between the maximum pressures and masses. Linear regression equations have been computed for the data and are shown as the solid lines in Figures 4 and 5. The regression equations are also given in Table 8. These equations are all of the form:

$$P_{max} = k_i m \qquad \text{Eq. 17}$$

where k_i is the slope of the maximum pressure with respect to the mass of a given propellant. Furthermore, a relationship between the slopes, k_i, and the vent area can be observed, as shown in Figure 6. From the analysis performed, the maximum pressure is estimated as

$$P_{max} = \frac{470m}{A} \qquad \text{Eq. 18}$$

for the DB1 cases. This empirical law is not satisfactory as its validity beyond the test conditions cannot be ensured. Such a simple relationship can, however, provide a way to compare with the following more complex analysis.

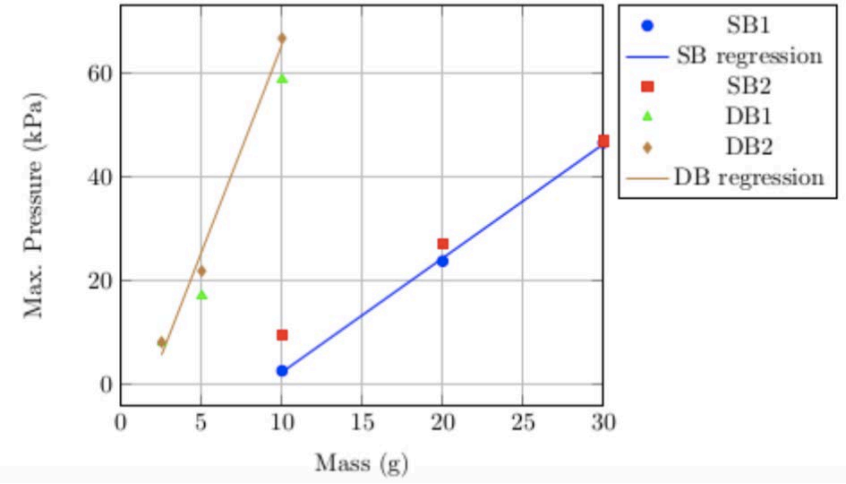

Figure 4: Maximum pressure as a function of the sample mass in the 60-L enclosure. The correlation coefficients, r^2, are 0.95 and 0.98 for the SB and DB data respectively.

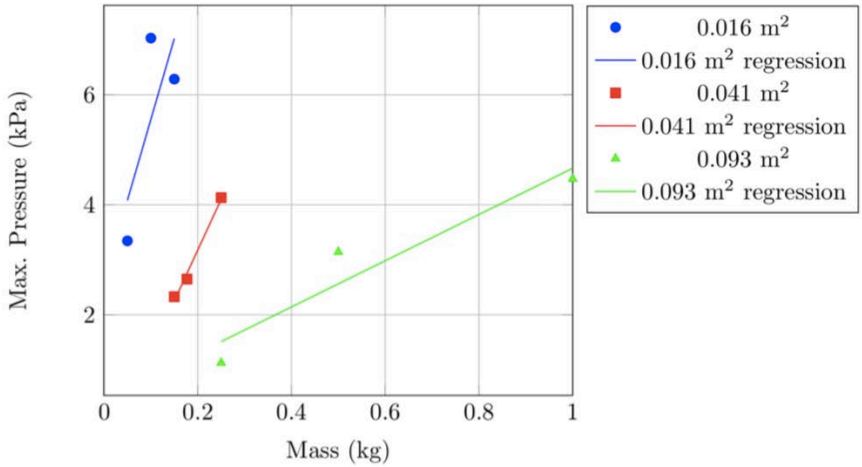

Figure 5: Maximum pressure as a function of the sample mass in the 1800-L enclosure. The correlation coefficients, r^2, are 0.60, 0.99 and 0.91 for the 0.016, 0.041 and 0.093 m^2 data respectively.

Table 8: Linear regression equations of the data shown on Figures 4 and 5.

Propellant	Volume (m^3)	Area (m^2)	Regression equation
SB1 and SB2	60 L	0.0007 m^2	$P_{max} = 1870m$
DB1 and DB2	60 L	0.0007 m^2	$P_{max} = 6970m$
DB1	1800 L	0.016 m^2	$P_{max} = 29.4m$
DB1	1800 L	0.041 m^2	$P_{max} = 18.5m$
DB1	1800 L	0.093 m^2	$P_{max} = 4.2m$

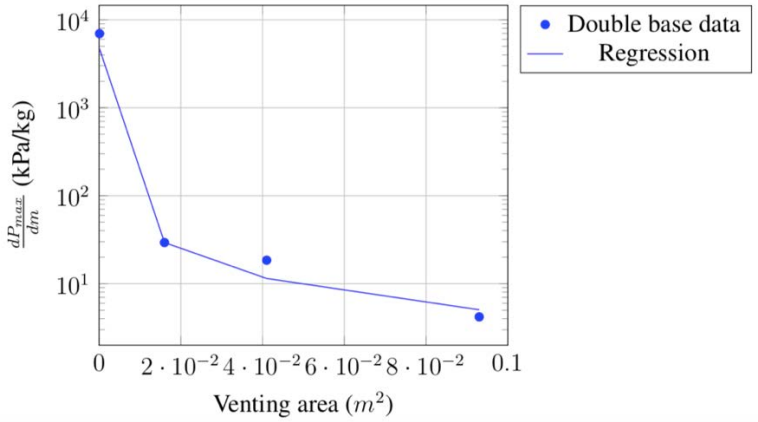

Figure 6: Maximum pressure rate of change with respect to mass as a function of the venting area for DB1. The correlation coefficient, r^2, is 0.99 for this data.

The general model form obtained through theoretical considerations, given as Eq. 11, is helpful in going forward in optimizing the model. This form and the previous conclusions indicate that the new model should look as follows:

$$P_{max} = k\, m^{a_1} A^{a_2} \qquad \text{Eq. 19}$$

where *k* is an empirical constant. By taking the logarithm on both sides of Eq. 19 and simplifying, a linear relationship with the unknown constants is obtained.

$$\log P_{max} = \log k + a_1 \log m + a_2 \log A \qquad \text{Eq. 20}$$

The method of multiple linear regressions was applied on the data using the R statistical code through the R-Studio interface (R core Team 2013). The following regression model was obtained:

- When considering the following variables for DB1: mass and venting area:

$$P_{max} = \frac{194.6\, m^{0.97}}{A^{1.34}} \qquad \text{Eq. 21}$$

- The regression line fits the data with a correlation coefficient $r^2 = 0.91$.

The interpretation of this last result must, however, be made carefully. Eq. 21 is seen to not follow the expected inverse square relationship for the area. If the inverse square relationship is forced in the regression, the fits are unacceptable. Two important observations must be made about the situation:

- The group of points (shown in Figure 7) is mostly within the uncertainty region between the error limits.

- The range of areas tested is relatively small (there is a factor of 6 between the extreme values in the 1800-L enclosure). Over such a small range, an inverse square relationship can be simplified as a direct inverse. Testing with larger areas is not practical as pressures become very low. Extending to smaller areas becomes problematic as pressures would rise to dangerously high levels (unless impractically small masses were used). The tested range was thus in the right location with respect to the intended application.

- The resulting expression does not take into account any change in the thermodynamic variables and discharge coefficient.

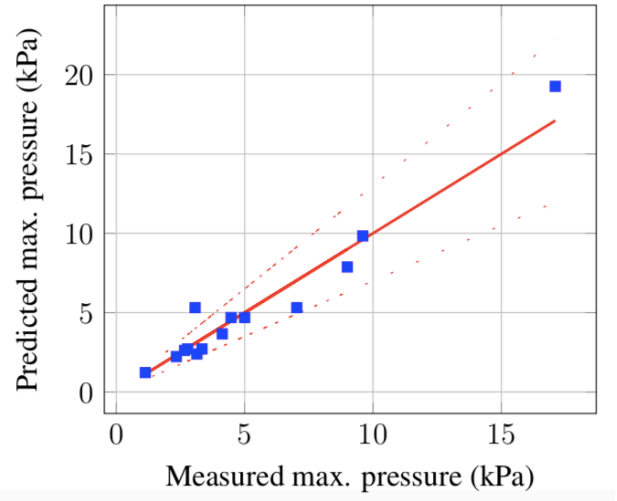

Figure 7: Comparison of the measured and predicted maximum pressures calculated using the best statistical model. Note that the solid line has the desired unity slope.

This is a classic issue when performing a statistical regression on experimental data. The best regression model does not necessarily reflect the ultimate best model. What can be said is the following: the best regression model, Eq. 21, represents the best fit for these variables in their tested range.

The inverse square area model has a theoretical background and is used in other cases. It should be expected to better predict the pressure in applications of various scales. By comparing the two models, it is possible to estimate the variation of the discharge coefficient with the venting area. The non-ideal behavior of fluid flow through restriction is such that the mass flow rate is smaller by a fraction equal to the discharge coefficient (Smith and Van Winkle 1958). This flow reduction can be modelled by considering an ideal flow through a smaller area. Furthermore, since the discharge coefficient is used directly in the mass flow rate expression (i.e., not raised by any power), it should have the same effect on the area. The area relationship can thus be seen as follows:

$$\frac{1}{(C_D A)^{1.34}} \approx \frac{1}{A^2} \qquad \text{Eq. 22}$$

Here, $C_D = f(A)$ and thus varies such that its effect results in the desired inverse square relationship. Solving for the discharge coefficient yields the simple result:

$$C_D \approx A^{1/2} \qquad \text{Eq. 23}$$

The previous result must, however, be used carefully as C_D usually takes values between 0 and 1. It can be seen that for the largest area tested (0.093 m^2), a resulting C_D = 0.31 is obtained. As the area is increased above 1 m^2, the predicted discharge coefficient would go above unity. In reality, it is expected that C_D will increase to an asymptotic maximum value located between 0.70 and 0.90 (Smith and Van Winkle 1958). It can be concluded that the obtained

model does follow the inverse square law as long as the variable nature of the state variables and discharge coefficient is recognized. If the pressure generation is modelled numerically, a further adjustment would be necessary to decouple the effect of the thermodynamic state variables and that of the discharge coefficient. This last conclusion is discussed further next, along with the issue of scale change, through the aid of a numerical tool.

3.4 Scale considerations

As it is the case with most empirical models, it is expected that a change of application scale results in a change in the state variable values. To help account for the effect of scale, a numerical solution of Eq. 8 was used. In the previous introduction of the pressure evolution model, it was shown that a lumped parameter approximation is sufficient. Therefore, one only needs to use Eq. 8 with a finite time interval, Δt, to obtain a numerical solution. A time evolution of the pressure is obtained by iterating the solution back as part of the inputs.

In all of the previous derivations, most thermodynamic parameters, such as temperature and density, were assumed to be constant. This assumption simplifies the calculation of the maximum pressure. In a numerical solution, these thermodynamic parameters can, however, be taken as variables. The solution for these new variables is obtained through an energy balance relation and the application of a proper equation of state. In the present case, the energy balance consists of two terms: an energy input due to the heat of combustion (heat of explosion) and an energy output due to the kinetic energy and enthalpy of the gases escaping from the vent opening. The energy balance equation is thus as follows:

$$\Delta T = \frac{\dot{m}_{gen}\, E\, \Delta t - C_v\, \dot{m}_{vent}\, T\, \Delta t}{C_v(m_{air} - \rho_{gas} V)} \qquad \text{Eq. 24}$$

where the energy output term, second term of the numerator, accounts for the kinetic energy and enthalpy of the exhausting gases. The energy balance equation yields a temperature difference at every time step. The gas density can then be computed from the ideal gas equation of state as follows:

$$\rho_{gas} = \frac{P M_w}{RT} \qquad \text{Eq. 25}$$

Starting from the standard conditions with a known combustion rate relationship, it is possible to increment the pressure, temperature and density at each step. These new results are iterated in the equations for the next time step and the process is repeated. Calculations can stop when the correct fuel mass has burned and the pressure is back at atmospheric value. For any numerical solution, the stability of the solution is important. In this case, selecting the right time step, is imperative in ensuring this stability. An adaptive time step algorithm was used to determine an optimal increment size for each calculation step (Gilat and Subramaniam 2013). This algorithm checks the effect of changing the time step size on the solution and selects the largest increment that keeps the solution stable within a certain defined error bound. Comparing the results of the numerical calculations with the previously presented experimental data yields what is shown on Figure 8.

The effect of scale can thus be studied by considering the case of a 100 m^3 room containing 50 kg of double bass propellant (DB1). Although this case was not the subject of an experimental test, its analysis using the numerical tool is instructive. Interestingly, similar quantities were studied in the irradiance analysis section. These tests showed a steady state time of around 4-5 s, thus yielding a combustion rate $\dot{m}_{gen} \approx 20$ kg/s. Applying these values, along with a 0.5 m^2 vent opening, yields a maximum pressure of 2.7 kPa. The resulting densities and temperatures of all tested scales are shown in Table 9.

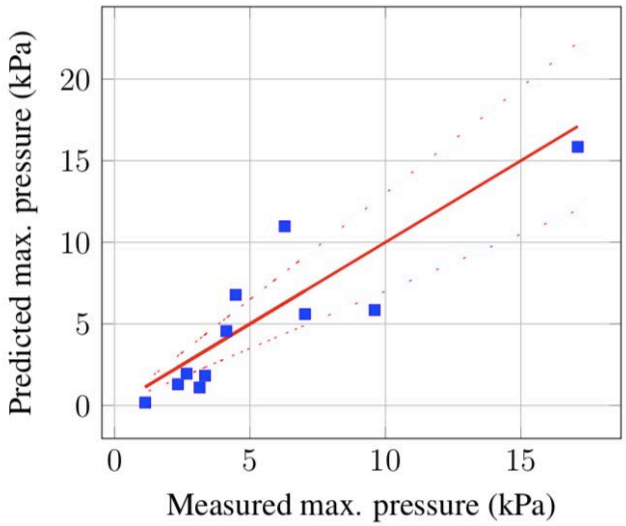

Figure 8: Comparison of the measured and predicted maximum pressures calculated using numerical solutions of the pressure evolution equation.

Table 9: Summary of the calculated average minimum densities and maximum temperatures.

Volume (m^3)	Min. density (kg/m^3)	Max. Temperature (K)	Mass ratio (s^{-1})
0.06	0.74	452	0.2
1.8	0.48	823	0.5
100	0.18	1798	0.2

Interestingly, regression analysis yields the following expression for density with the DB1 cases (with a correlation coefficient, r^2, of 0.97):

$$\rho_{gas} = 0.47V^{-0.19} \qquad \text{Eq. 26}$$

Substituting in the theoretical expression for maximum pressure and simplifying yields:

$$P_{max} = \frac{1.06\,\dot{m}^2\,V^{0.19}}{C_D^2\,A^2} \qquad \text{Eq. 27}$$

where the discharge coefficient value derived previously, $C_D = A^{1/2}$, cannot be applied as the variation in density is part of this equation. By regression, one can find that the optimal discharge coefficient would here be $C_D = A^{1/3}$,. The resulting equation thus becomes:

$$P_{max} = \frac{1.06\,\dot{m}^2\,V^{0.19}}{A^{2.66}} \qquad \text{Eq. 28}$$

This expression is therefore valid for cases with a venting area below 0.5 m^2, as long as the pressure remains within the tested range of 0 to 10 kPa. For larger scale configurations involving venting area above 0.5 m^2, a constant discharge coefficient of 0.80 is assumed and the following is applied:

$$P_{max} = \frac{1.66\,\dot{m}^2\,V^{0.19}}{A^2} \qquad \text{Eq. 29}$$

The previous three equations are valid for the DB1 case. A change in propellant type would be reflected on the combustion rate and the constant factor. As was done previously, the numerical code could be used to calculate the constant factors of other propellants (that calculation would take into consideration the changes in thermodynamical variables and heat release rate). A graphical comparison of DB1 measured and predicted values is shown in Figure 9. As expected, the fit is not as optimal as a statistical inverse area model (Eq.~\eqref{eq:p10921x12}) but the present expression is the more general version.

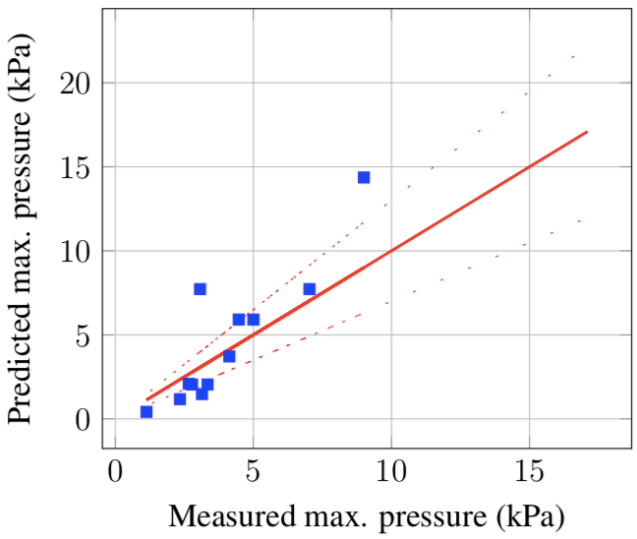

Figure 9: Comparison of the measured and predicted maximum pressures calculated using the scale dependant model. Note that the solid line has the desired unity slope.

4. Conclusion

This study focuses on the analysis of a series of tests in which the pressure was measured during propellant fires in two vented enclosures. Two useful conclusions were drawn concerning the maximum pressures and the maximum rates of pressure rise obtained in such events. These conclusions are in the form of empirical laws valid within the tested conditions. Another, more general, conclusion concerns the initial part of the fire when flames are still propagating on the surface of the propellant bed. One can define an induction time for this part of the event and estimate that time as the initial nonlinear part of the pressure curve. The test data shows a dependence of the induction time on the diameter (or surface area) of the propellant stack.

An analysis of the present results and conclusions with respect to theoretical considerations provides further insight in the observed behaviors. This analysis looks at these events with the help of thermodynamics and gas dynamics. The results are more general estimation tools, in the form of semi-empirical laws and numerical models. Special care must however be taken in using these models as it is necessary to have a good estimate of the mass burning rate of the configuration under study. The general relationships derived in this study can already be applied to many cases encountered in the propellant industry. With the addition of prediction tools for flame propagation and radiant heat flux, designers will be able to build facilities that provide a better fire safety.

5. References

Amyotte, Paul. 2013. *An Introduction to Dust Explosions: Understanding the Myths and Realities of Dust Explosions for a Safer Workplace*. Butterworth-Heinemann.

Carlucci, Donald E. and Jacobson, Sydney S. 2013. *Ballistics: Theory and Design of Guns and Ammunition, Second Edition*. CRC Press.

Cengel, Yunus A. and Boles, Michael A. 2014. *Thermodynamics, an engineering approach – 8th edition*, McGraw Hill.

Eckhoff, Rolf K. 2005. *Explosion Hazards in the Process Industries*. Gulf Publishing Company.

Frauenfelder, R. 1983. "Testing of a new concept for the storage of granular propellant". *Propellants, Explosives, Pyrotechnics*, 8(4):102–108.

Gilat, Amos and Subramaniam, Vish. 2013. *Numerical Methods for Engineers and Scientists – 3rd Edition*. Wiley.

Graham, Kenneth J. 1986. "Explosive Response to Fragments: Venting Studies". Naval Weapons Center, China Lake, California.

Joachim, Charles E. 1991. "Phase C, M-1 Propellant Tests: Deflagration in Partial Confinement". *Technical Report SL-91-11*, USAE Waterways Experiment Station, Structural Laboratory.

John, James E. A. and Keith, Theo G. 2006. *Gas Dynamics*. Pearson Prentice Hall.

Merrifield, Roy and Myatt, Stuart. 1998. "The risks associated with the storage of small quantities of gunpowder and shooters powders in containers and buildings". In *Proceedings of the 28th DOD Safety Seminar*, Orlando, Florida.

National Fire Protection Association. 2010. "NFPA 68: standard on explosion protection by deflagration venting, 2007 edition". *National Fire Protection Association*.

Paquet, Frederick. 2017. "The Fire Safety of Granular Propellant Handling Facilities". PhD diss., Concordia University, Montreal, Quebec, Canada.

Polcyn, Michael A. and Mullin, Scott A. 1998. "Propellant loads testing application to facility design". In *Proceedings of the 28th DOD Safety Seminar*, Orlando, Florida.

Porterie, Bernard, Larini, Michel, Giroud, F. and Loraud, J.C. 1996. "Solid-propellant fire in an enclosure fitted with a ceiling safety-vent". *International Journal of Heat and Mass Transfer*, 39(3):575–601.

R Core Team. 2013. "R: A Language and Environment for Statistical Computing". *R Foundation for Statistical Computing*, Vienna, Austria.

Racette, Mathieu, Brousseau, D. and Valliere, C. 2004. "Rapport d'essais - transition de deflagration a detonation". *Technical Report CEEM04-067*, Centre d'essais et d'experimentation en munition, Val Cartier, Quebec.

Smith, P.L. and Van Winkle, Matthew. 1958. "Discharge coefficients through perforated plates at reynolds numbers of 400 to 3,000". *AIChE Journal*, 4(3):266–268.

Taylor, John R. 1997. *An Introduction to Error Analysis: The Study of Uncertainties in Physical Measurements"*. University Science Books.

Wharton, Roland K., Formby, Stuart A. and Merrifield, Roy. 2001. "Airblasts TNT equivalence for a range of commercial blasting explosives". *J. Hazard. Mater.*, 79(1-2):31–39.

White, Derek A., Beyler, Craig L., Williams, Frederick W. and Tatem, Patricia A. 2000. "Modeling missile propellant fires in shipboard compartments". *Fire Saf. J.*, 34(4):321– 341.